TSINGHUA SCIENCE AND TECHNOLOGY
ISSN 1007-0214 03/19 pp520-526
Volume 12, Number 5, October 2007

BEM Analysis of Wave Propagation in a Water-Filled Borehole in an Anisotropic Solid

S. Hirose**, Y. Ushida, C. Y. Wang†

**Department of Mechanical and Environmental Engineering,
Tokyo Institute of Technology, Tokyo 152-8552, Japan;
† Schlumberger-Doll Research, 36 Old Quarry Road, Ridgefield, CT 06877-4108, USA**

Abstract: This paper describes a time-domain boundary element method developed to analyze the interactions of acoustic and elastic waves near the interfaces between water and an anisotropic elastic solid. Two models are analyzed with one being the interface between two half spaces of fluid and solid and the other being a fluid region sandwiched by half space domains of anisotropic elastic solids. Both monopole and dipole point sources are used to generate an initial pressure wave in the fluid. Some snapshots of the transient wave behavior near the fluid-solid interfaces are given. The effect of the anisotropy in the solid on the pressure waveforms in the fluid is discussed. The numerical results allow detailed arrival identification and interpretation of acoustic and elastic waves propagating along the fluid-solid interfaces.

Key words: boundary element method; wave propagation; anisotropic solid; fluid-solid interface

Introduction

Sonic measurements are important techniques used to estimate the mechanical properties of rocks for efficient and safe production of oil and gas[1]. In sonic measurements, acoustic waves are excited and received in a fluid-filled borehole surrounded by rock, with the waveforms analyzed to determine the rock properties from the wave velocity, amplitude, and dispersion. Acoustic waves propagating in a borehole are guided waves with complicated behavior due to the interaction between the fluid and the rock. Sonic logging measurements require wave analysis of fluid-solid interactions. Many numerical wave analysis studies of sonic measurements have been done, mostly using finite difference methods[2-5]. In this paper, a time-domain boundary element method (BEM) is used to analyze the interaction between acoustic and elastic waves around a borehole in anisotropic elastic media. The fundamental solutions for a general anisotropic elastic solid derived by Wang and Achenbach[6] are utilized in the BEM calculations.

1 Problem Statement

The two two-dimensional (2-D) models shown in Fig. l are considered in this paper. One is a simple interface between two half spaces of fluid and an anisotropic elastic solid. The other is a model of fluid sandwiched between anisotropic elastic solids. The first model shown in Fig. 1 is investigated to study the basic transient behavior of the reflection and transmission of acoustic waves at the fluid-solid interface, while the second model is considered to investigate the dispersive properties of guided waves propagating in the fluid region, as a 2-D model of a fluid-filled borehole. The incident wave is excited by a point source in the fluid. Both monopole and dipole point sources are considered. The analysis assumes that the normal

Received: 2007-03-15
** To whom correspondence should be addressed.
E-mail: shirose@cv.titech.ac.jp

components of displacement and traction on the interfaces are continuous and the tangential traction components are zero.

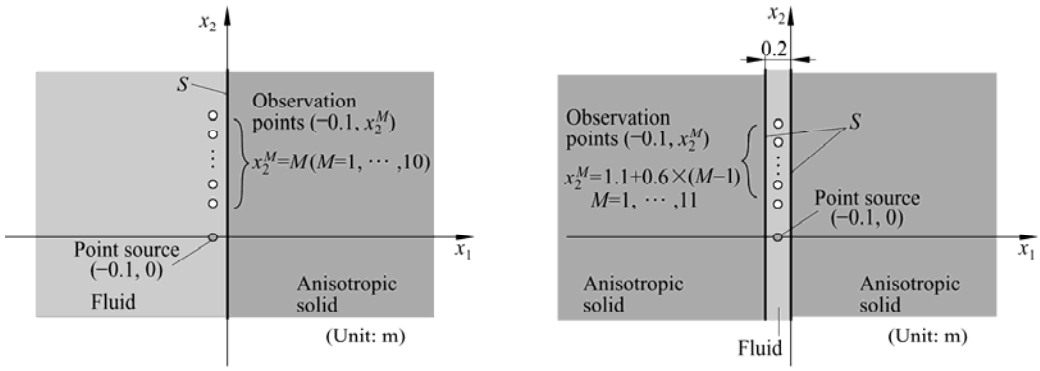

Fig. 1 Two 2-D models

2 Governing Equations

Let D_s and D_f represent the anisotropic elastic solid and fluid domains. The displacement $\boldsymbol{u}$ in a two-dimensional anisotropic solid D_s satisfies the equations of motion

$$\left\{\Gamma_{ij}(\partial_1,\partial_2)-\rho_s\delta_{ij}\partial_t^2\right\}u_j(\boldsymbol{x},t)=0 \quad \text{for } \boldsymbol{x} \text{ in } D_s \tag{1}$$

where $\Gamma_{ij}(\partial_1,\partial_2)=C_{i\alpha j\beta}\partial_\alpha\partial_\beta$ and $C_{i\alpha j\beta}$ are elastic constants and ρ_s is the mass density. The pressure p in fluid D_f satisfies

$$\left\{\partial_\beta\partial_\beta-c_f^{-2}\partial_t^2\right\}p(\boldsymbol{x},t)=0 \quad \text{for } \boldsymbol{x} \text{ in } D_f \tag{2}$$

where c_f is the acoustic wave velocity in the fluid. Equations (1) and (2) are connected in the analysis by the continuity and boundary conditions on the interface S between the fluid and solid as follows.

$$\begin{aligned} -p=\boldsymbol{n}\cdot\boldsymbol{\tau}, \quad -\partial p/\partial\boldsymbol{n}=\rho_f\boldsymbol{n}\cdot\partial_t^2\boldsymbol{u}, \\ \boldsymbol{s}_1\cdot\boldsymbol{\tau}=\boldsymbol{s}_2\cdot\boldsymbol{\tau}=0 \quad \text{on } S \end{aligned} \tag{3}$$

where $\boldsymbol{\tau}$ is the traction vector, ρ_f is the fluid mass density, and $\boldsymbol{n}, \boldsymbol{s}_1, \boldsymbol{s}_2$ are the normal vector, the in-plane and the anti-plane tangential vectors on the interface, respectively.

3 Boundary Integral Equations

With a zero initial condition, the elastic wave fields in an anisotropic solid satisfy the following time-domain boundary integral equations[7].

$$\begin{aligned} \int_S\left\{\boldsymbol{U}_{nj}^S(\boldsymbol{x},\boldsymbol{y})\boldsymbol{\tau}_n(\boldsymbol{x},t)+\boldsymbol{U}_{nj}^R(\boldsymbol{x},\boldsymbol{y};t)\bullet\dot{\boldsymbol{\tau}}_n(\boldsymbol{x},t)\right\}ds_x - \\ p.v.\int_S\left\{T_{ij}^S(\boldsymbol{x},\boldsymbol{y})u_i(\boldsymbol{x},t)+T_{ij}^R(\boldsymbol{x},\boldsymbol{y};t)\bullet\dot{u}_i(\boldsymbol{x},t)\right\}ds_x = \\ c_{ij}(\boldsymbol{y})u_i(\boldsymbol{y},t) \quad \text{for } \boldsymbol{y} \text{ on } S \end{aligned} \tag{4}$$

where $\boldsymbol{\tau}_n$ is the normal component of traction and the last two boundary conditions in Eq. (3) are implemented. In Eq. (4), the dots stand for the time derivative, *p.v.*stands for the principal value of the integral and the asterisk stands for the time convolution integral, respectively, and $c_{ij}(\boldsymbol{y})$ is the so-called free term depending on the geometry at the boundary point $\boldsymbol{y}$. Also, U_{ij} and T_{ij} are fundamental solutions for the anisotropic solid and the superscripts S and R denote the static singular part and the dynamic regular part. The components of the fundamental solutions are explicitly given as[6]:

$$\begin{aligned} U_{ij}^S(\boldsymbol{x},\boldsymbol{y})&=\frac{1}{\pi}\Im\sum_{m=1}^M\left[\frac{A_{ij}(\eta_m)}{\partial_\eta D(\eta_m)}\log(z_m)-\log(\eta_m+i)\right], \\ U_{ij}^R(\boldsymbol{x},\boldsymbol{y},t)&=\frac{H(t)}{4\pi^2}\int_{|\boldsymbol{e}|=1}\sum_{m=1}^M\frac{P_{ij}^m}{\rho_s c_m^2}\frac{d\boldsymbol{e}}{c_m t+\boldsymbol{e}\cdot(\boldsymbol{x}-\boldsymbol{y})} \\ T_{ij}^S(\boldsymbol{x},\boldsymbol{y})&=\frac{1}{\pi}\frac{\partial}{\partial s_x}\Im\sum_{m=1}^M\left[\frac{B_{ij}(\eta_m)}{\partial_\eta D(\eta_m)}\log(z_m)\right], \\ T_{ij}^R(\boldsymbol{x},\boldsymbol{y},t)&=\frac{H(t)}{4\pi^2}\int_{|\boldsymbol{e}|=1}\sum_{m=1}^M\frac{Q_{ij}^m}{\rho_s c_m^3}\log|c_m t+\boldsymbol{e}\cdot(\boldsymbol{x}-\boldsymbol{y})|\,d\boldsymbol{e} \end{aligned} \tag{5, 6}$$

In the static singular parts of $U_{ij}^S(\boldsymbol{x},\boldsymbol{y})$ and $T_{ij}^S(\boldsymbol{x},\boldsymbol{y})$, $A_{ij}(\eta)=\text{adj}[\Gamma_{ij}(1,\eta)]$, $B_{ij}(\eta)=(C_{i2p1}+C_{i2p2}\eta)A_{pj}(\eta)$, $D(\eta)=\det[\Gamma_{ij}(1,\eta)]$, $z_m=x_1+\eta_m x_2$, η_m is the root of $D(\eta_m)=0$ with the positive imaginary part and

$\partial / \partial s_x$ denotes the tangential derivative at the point $\boldsymbol{x}$. In the dynamic parts of $U_{ij}^{\mathrm{R}}(\boldsymbol{x},\boldsymbol{y},t)$ and $T_{ij}^{\mathrm{R}}(\boldsymbol{x},\boldsymbol{y},t)$, $P_{ij}^{m}=\boldsymbol{E}_{im}\boldsymbol{E}_{jm}$ and $Q_{ij}^{m}=C_{i\alpha p\beta}n_{\alpha}(\boldsymbol{x})e_{\beta}P_{pj}^{m}(\boldsymbol{e})$, where $\boldsymbol{E}_{im}$ and $\rho_s c_m^2$ are the m-th eigenvector and eigenvalue of the matrix $\boldsymbol{\Gamma}_{ij}(e_1,e_2)$.

For the pressure field in the fluid, the boundary integral equations are[8]

$$p^{\mathrm{in}}(\boldsymbol{y},t)+\int_S P(\boldsymbol{x},\boldsymbol{y};t)\bullet\frac{\partial p}{\partial \boldsymbol{n}'}(\boldsymbol{x},t)\mathrm{d}s_y+ p.v.\int_S Q(\boldsymbol{x},\boldsymbol{y};t)\bullet\dot{p}(\boldsymbol{x},t)\mathrm{d}s_y= c'(\boldsymbol{y})p(\boldsymbol{y},t)\quad \text{for } \boldsymbol{y} \text{ on } S \tag{7}$$

where P and Q are the following well known fundamental solutions for acoustic waves:

$$P(\boldsymbol{x},\boldsymbol{y},t)=\frac{H(t-r/c_{\mathrm{f}})}{2\pi\sqrt{t^2-(r/c_{\mathrm{f}})^2}}$$

and

$$Q(\boldsymbol{x},\boldsymbol{y},t)=\frac{1}{2\pi r}\frac{\partial r}{\partial \boldsymbol{n}'(\boldsymbol{x})}\frac{tH(t-r/c_{\mathrm{f}})}{\sqrt{t^2-(r/c_{\mathrm{f}})^2}} \tag{8}$$

where $r=|\boldsymbol{x}-\boldsymbol{y}|$ and $\partial/\partial\boldsymbol{n}'$ is the derivative with respect to the outward normal from the fluid forwards to the solid.

In Eq. (7), p^{in} is the incident pressure emitted from a monopole or dipole point source in the fluid. The incident pressure field p^{in} can be expressed as

$$p^{\mathrm{in}}(\boldsymbol{y},t)=\begin{cases}-\rho_{\mathrm{f}}\ddot{v}_0(\boldsymbol{z}_0,t)\bullet P(\boldsymbol{y},\boldsymbol{z}_0,t) & \text{for monopole source;}\\ \dot{\boldsymbol{\tau}}_0(\boldsymbol{z}_0,t)\bullet Q(\boldsymbol{y},\boldsymbol{z}_0,t) & \text{for dipole source}\end{cases} \tag{9}$$

where v_0 is the time variation of the volume change of a monopole source and $\boldsymbol{\tau}_0$ is the traction at a dipole source. In the numerical examples shown later, v_0 and $\boldsymbol{\tau}_0$ are given as:

$$\left.\begin{matrix}-\rho_{\mathrm{f}}\ddot{v}_0(\boldsymbol{z}_0,t)\\ \boldsymbol{\tau}_0(\boldsymbol{z}_0,t)\end{matrix}\right\}=A_0\sin(2\pi t/T_0)H(t)H(N_0T_0-t) \tag{10}$$

where A_0 is the amplitude, T_0 is the period, and N_0 is the wave number of the sinusoidal source function.

Substituting the continuity condition in Eq. (3) into Eq. (7) yields

$$p^{\mathrm{in}}(\boldsymbol{y},t)+\int_S P(\boldsymbol{x},\boldsymbol{y};t)\bullet\rho_{\mathrm{f}}\ddot{u}_{\mathrm{n}}(\boldsymbol{x},t)\mathrm{d}s_y- p.v.\int_S Q(\boldsymbol{x},\boldsymbol{y};t)\bullet\dot{\boldsymbol{\tau}}_{\mathrm{n}}(\boldsymbol{x},t)\mathrm{d}s_y=-c'(\boldsymbol{y})\boldsymbol{\tau}_{\mathrm{n}}(\boldsymbol{y},t)$$

$$\text{for } \boldsymbol{y} \text{ on } S \tag{11}$$

where u_{n} is the normal component of the displacement and t_{n} is the traction in the solid.

Further assume that in the numerical calculations, linear interpolations are introduced for the time variations of the displacements on the boundary with constants for the tractions. Comparison of Eqs. (4) and (11) shows that the time variations of the displacement and traction in Eq. (11) are one order higher than those in Eq. (4). To use approximations of the same order in both equations, Eq. (11) is integrated with respect to time as

$$\int_0^t p^{\mathrm{in}}(\boldsymbol{y},\varsigma)\mathrm{d}\tau+\int_S P(\boldsymbol{x},\boldsymbol{y};t)\bullet\rho_{\mathrm{f}}\dot{u}_n(\boldsymbol{x},t)\mathrm{d}s_y- p.v.\int_S Q(\boldsymbol{x},\boldsymbol{y};t)\bullet\dot{g}_{\mathrm{n}}(\boldsymbol{x},t)\mathrm{d}s_y=-c'(\boldsymbol{y})g_{\mathrm{n}}(\boldsymbol{y},t)$$

$$\text{for } \boldsymbol{y} \text{ on } S \tag{12}$$

where $g_{\mathrm{n}}(\boldsymbol{x},t)=\int_0^t\boldsymbol{\tau}_{\mathrm{n}}(\boldsymbol{y},\varsigma)\mathrm{d}\varsigma$. By using g_{n} instead of $\boldsymbol{\tau}_{\mathrm{n}}$, Eq. (4) is rewritten as

$$\int_S\left\{\boldsymbol{U}_{\mathrm{nj}}^{\mathrm{S}}(\boldsymbol{x},\boldsymbol{y})\dot{g}_{\mathrm{n}}(\boldsymbol{x},t)+\boldsymbol{U}_{\mathrm{nj}}^{\mathrm{R}}(\boldsymbol{x},\boldsymbol{y};t)\bullet\ddot{g}_n(\boldsymbol{x},t)\right\}\mathrm{d}s_x- p.v.\int_S\left\{T_{ij}^{\mathrm{S}}(\boldsymbol{x},\boldsymbol{y})u_i(\boldsymbol{x},t)+T_{ij}^{\mathrm{R}}(\boldsymbol{x},\boldsymbol{y};t)\bullet\ddot{u}_i(\boldsymbol{x},t)\right\}\mathrm{d}s_x= c_{ij}(\boldsymbol{y})u_i(\boldsymbol{y},t)\quad \text{for } \boldsymbol{y} \text{ on } S \tag{13}$$

Introducing constant and linear approximations for the spatial variations and linear approximations for the temporal variations in both u_i and g_{n}, then Eqs. (12) and (13) can be written in discretized matrix forms as:

$$\boldsymbol{C}\boldsymbol{u}_K=\boldsymbol{U}^{\mathrm{S}}(\boldsymbol{g}_K-\boldsymbol{g}_{K-1})/\Delta t-\boldsymbol{T}^{\mathrm{S}}\boldsymbol{u}_K+\sum_{k=1}^{K}\left[\boldsymbol{U}_{K-k+1}^{\mathrm{R}}\boldsymbol{g}_k-\boldsymbol{T}_{K-k+1}^{\mathrm{R}}\boldsymbol{u}_k\right] \tag{14}$$

$$-\boldsymbol{C}'\boldsymbol{g}_{n,K}=\boldsymbol{q}_K^{\mathrm{in}}+\sum_{k=1}^{K}\left[\boldsymbol{P}_{K-k+1}\boldsymbol{u}_{n,k}-\boldsymbol{Q}_{K-k+1}\boldsymbol{g}_{n,k}\right] \tag{15}$$

where K is the current time step and k is the index for time convolution, Δt is the time increment and $\boldsymbol{q}_K^{\mathrm{in}}$ denotes the discretized term for the first integral on the left hand side of Eq. (12). Note that in Eq. (13), the second order derivatives in time behave like a delta function since linear interpolation functions were used for the temporal variations of u_i and g_{n}. Therefore, the time convolutions including $\ddot{u}_i$ and $\ddot{g}_{\mathrm{n}}$ are evaluated analytically.

After collecting all unknown terms at the current time step K on the left hand side, Eqs. (14) and (15) are written in matrix form as

$$\begin{bmatrix} \boldsymbol{T}_{\mathrm{nn}} & \boldsymbol{T}_{\mathrm{n}s_1} & \boldsymbol{T}_{\mathrm{n}s_2} & -\boldsymbol{U}_{\mathrm{nn}} \\ \boldsymbol{T}_{s_1\mathrm{n}} & \boldsymbol{T}_{s_1s_1} & \boldsymbol{T}_{s_1s_2} & -\boldsymbol{U}_{s_1\mathrm{n}} \\ \boldsymbol{T}_{s_2n} & \boldsymbol{T}_{s_2s_1} & \boldsymbol{T}_{s_2s_2} & -\boldsymbol{U}_{s_2\mathrm{n}} \\ -\boldsymbol{P}_1 & \boldsymbol{0} & \boldsymbol{0} & -\boldsymbol{C}'+\boldsymbol{Q}_1 \end{bmatrix} \begin{Bmatrix} \boldsymbol{u}_{n,K} \\ \boldsymbol{u}_{s_1,K} \\ \boldsymbol{u}_{s_2,K} \\ \boldsymbol{g}_{\mathrm{n},K} \end{Bmatrix} = \begin{Bmatrix} \boldsymbol{f}_{\mathrm{n},K} \\ \boldsymbol{f}_{s_1,K} \\ \boldsymbol{f}_{s_2,K} \\ \boldsymbol{h}_K \end{Bmatrix} \quad (16)$$

where the subscripts n, s_1, and s_2 are the normal and two tangential directions and

$$\boldsymbol{T} = \boldsymbol{C} + \boldsymbol{T}^{\mathrm{S}} + \boldsymbol{T}_1^{\mathrm{R}}, \quad \boldsymbol{U} = \boldsymbol{U}^{\mathrm{S}}/\Delta t + \boldsymbol{U}_1^{\mathrm{R}},$$

$$\boldsymbol{f}_K = \sum_{k=1}^{K-1}\left[\boldsymbol{U}_{K-k+1}^{\mathrm{R}}\boldsymbol{g}_k - \boldsymbol{T}_{K-k+1}^{\mathrm{R}}\boldsymbol{u}_k\right] - \boldsymbol{U}^{\mathrm{S}}\boldsymbol{g}_{K-1}/\Delta t \quad (17)$$

$$\boldsymbol{h}_K = \boldsymbol{q}_K^{\mathrm{in}} + \sum_{k=1}^{K-1}\left[\boldsymbol{P}_{K-k+1}\boldsymbol{u}_{\mathrm{n},k} - \boldsymbol{Q}_{K-k-1}\boldsymbol{g}_{\mathrm{n},k}\right] \quad (18)$$

Once $\boldsymbol{u}$ and g_{n} on the interface between the fluid and solid are determined by solving Eq. (16), the displacements in the solid and the pressure in the fluid can be calculated using the following integral equations.

$$\int_S \left\{\boldsymbol{U}_{\mathrm{n}j}^{\mathrm{S}}(\boldsymbol{x},\boldsymbol{y})\boldsymbol{\tau}_{\mathrm{n}}(\boldsymbol{x},t) + \boldsymbol{U}_{\mathrm{n}j}^{\mathrm{R}}(\boldsymbol{x},\boldsymbol{y};t)\bullet\dot{\boldsymbol{\tau}}_{\mathrm{n}}(\boldsymbol{x},t)\right\}\mathrm{d}s_x - p.v.\int_S \left\{T_{ij}^{\mathrm{S}}(\boldsymbol{x},\boldsymbol{y})u_i(\boldsymbol{x},t) + T_{ij}^{\mathrm{R}}(\boldsymbol{x},\boldsymbol{y};t)\bullet\ddot{u}_i(\boldsymbol{x},t)\right\}\mathrm{d}s_x = u_j(\boldsymbol{y},t) \quad \text{for } \boldsymbol{y} \text{ in } D_{\mathrm{s}} \quad (19)$$

$$p^{\mathrm{in}}(\boldsymbol{y},t) + \int_S P(\boldsymbol{x},\boldsymbol{y};t)\bullet\rho_{\mathrm{f}}\ddot{u}_{\mathrm{n}}(\boldsymbol{x},t)\mathrm{d}s_y - p.v.\int_S Q(\boldsymbol{x},\boldsymbol{y};t)\bullet\ddot{g}_{\mathrm{n}}(\boldsymbol{x},t)\mathrm{d}s_y = p(\boldsymbol{y}) \quad \text{for } \boldsymbol{y} \text{ in } D_{\mathrm{f}} \quad (20)$$

4 Numerical Examples

4.1 Fluid and elastic solid model

First consider the model of fluid and solid half spaces as shown in Fig. la. Figure 2 shows a snapshot of the acoustic and elastic waves near the interface at t=1.16 ms. The pressure amplitudes are plotted on the left halves of the figure with the displacements on the right half. The speed of sound in the fluid is given c_{f} =1500 m/s and the fluid density is ρ_{f} =1000 kg/m^3, and the solid is assumed to be transversely isotropic material with density $\rho_{\mathrm{s}} = 2000$ kg/m^3 and the following elastic constants:

$$\left[C_{ij}^{\mathrm{TI}}\right] = \begin{bmatrix} 24 & 3.2 & 8 & 0 & 0 & 0 \\ 3.2 & 32 & 3.2 & 0 & 0 & 0 \\ 8 & 3.2 & 24 & 0 & 0 & 0 \\ 0 & 0 & 0 & 12 & 0 & 0 \\ 0 & 0 & 0 & 0 & 8 & 0 \\ 0 & 0 & 0 & 0 & 0 & 12 \end{bmatrix} \quad (\times 10^9 \ \mathrm{N/m^2}) \quad (21)$$

The incident wave is excited by a dipole point source located at (–0.1, 0) [m], which has a sinusoidal time variation with T_0 =1 ms and N_0 =1. Figure 2 shows the wave fronts of the incident pressure wave and the head wave in the fluid related to the shear wave in the solid.

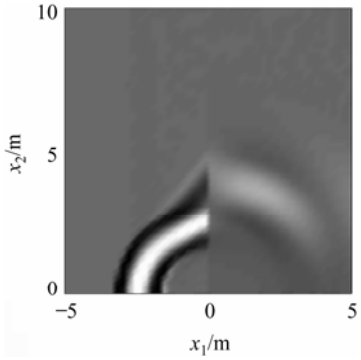

Fig. 2 Snapshot of acoustic and elastic waves near the interface of a fluid and an anisotropic solid at t=1.16 ms

Figure 3a shows the time variations of the fluid pressures at ten points of (–0.1, x_2^M) (x_2^M =1, ..., 10) [m] near the interface between the fluid and a transversely isotropic solid subjected to a time harmonic dipole point source with T_0 =1 ms and N_0 =3. Figure 3b shows the same figure as Fig. 3a, but with the solid as an isotropic material with the following elastic constants:

$$\left[C_{ij}^{\mathrm{Iso}}\right] = \begin{bmatrix} 24 & 8 & 8 & 0 & 0 & 0 \\ 8 & 24 & 8 & 0 & 0 & 0 \\ 8 & 8 & 24 & 0 & 0 & 0 \\ 0 & 0 & 0 & 8 & 0 & 0 \\ 0 & 0 & 0 & 0 & 8 & 0 \\ 0 & 0 & 0 & 0 & 0 & 8 \end{bmatrix} \quad (\times 10^9 \ \mathrm{N/m^2}) \quad (22)$$

Figure 4 shows the transient fluid pressure behavior for the same conditions as in Fig. 3, but with T_0 = 1/3 ms as the period for the dipole source function. Figure 5 shows the same results as Fig. 3, but for a monopole point source with T_0 =1 ms. In these figures, the numbers in the ordinates indicate the position index M of the observation points (–0.1, x_2^M). Comparison of parts (a) and (b) in Figs. 3 and 4 shows that for the dipole source, wave dispersion and attenuation are enhanced by the anisotropy of the solid which has a

higher wave speed in the vertical direction than in the horizontal direction. Comparison of Figs. 3 and 5 shows that the dipole source method is more sensitive to changes of the anisotropy than the monopole source method.

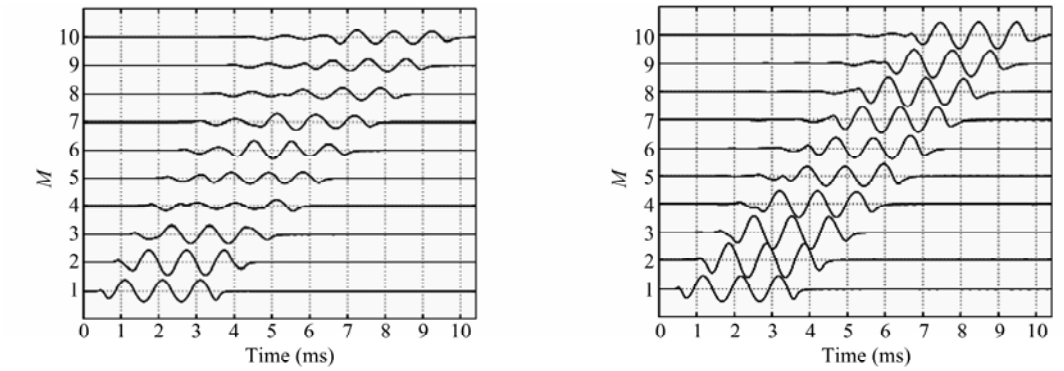

(a) Interface between a fluid and a transversely isotropic solid (b) Interface between a fluid and an isotropic solid

Fig. 3 Time variations of fluid pressures at ten observation points near the interface between a fluid and (a) a transversely isotropic solid and (b) an isotropic solid. The source is a dipole with T_0 =1 ms.

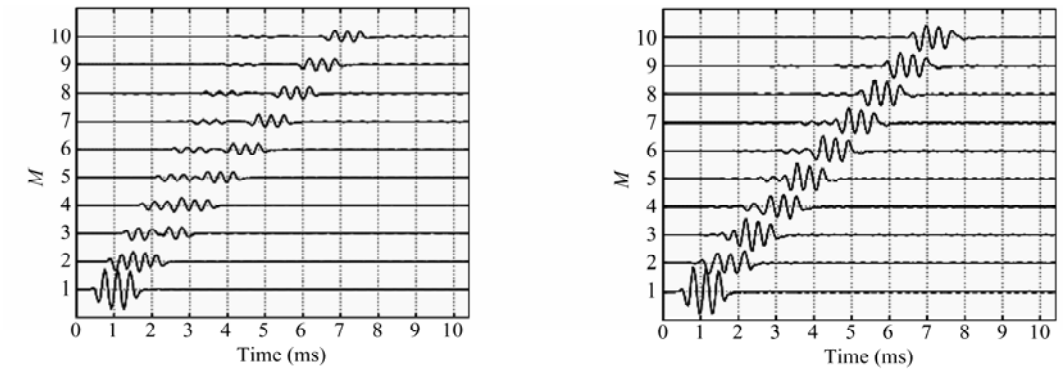

(a) Interface between a fluid and a transversely isotropic solid (b) Interface between a fluid and an isotropic solid

Fig. 4 Time variations of the fluid pressures at ten observation points near the interface between a fluid and (a) a transversely isotropic solid and (b) an isotropic solid. The source is a dipole with T_0 =1/3 ms.

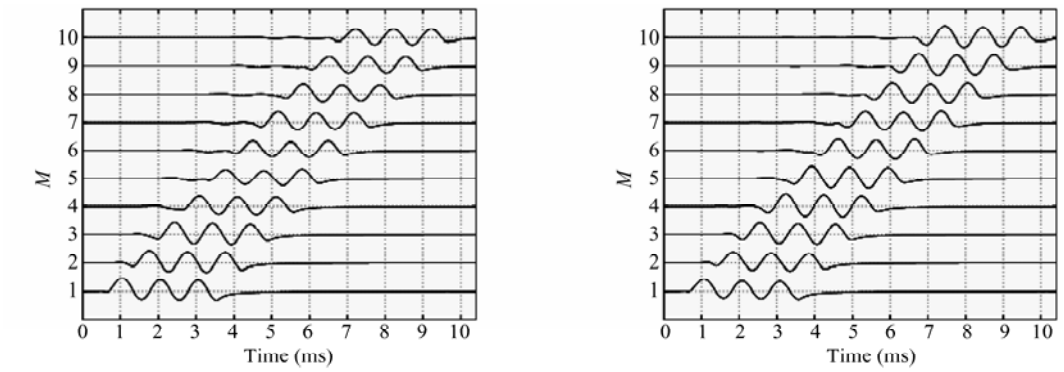

(a) Interface between a fluid and a transversely isotropic solid (b) Interface between a fluid and an isotropic solid

Fig. 5 Time variations of fluid pressures at ten observation points near the interface between a fluid and (a) a transversely isotropic solid and (b) an isotropic solid. The source is a monopole with T_0 =1 ms.

4.2 Solid-fluid-solid model

The second example has a fluid sandwiched between anisotropic elastic solids as shown in Fig. 1b. The width of the fluid-filled borehole is 0.2 m and the dipole source with a sinusoidal time variation with

T_0 =0.2 ms and N_0 =3 is located at (−0.1, 0). The fluid and anisotropic solid material constants are the same as for Fig. 2. Figure 6 shows snapshots of the acoustic and elastic waves around the dipole point source at several time steps. The oscillatory wave behavior in both the fluid and the solid are related to the time-dependent harmonic source. Note that the elastic waves in the solid propagate non-uniformly due to the anisotropy.

Figure 7 shows the time variations of the pressure calculated at the interior points of $\left(-0.1, x_2^M\right)$, where $x_2^M = 1.1 + 0.6(M-1)$ for $M = 1,\ldots,11$, in the fluid sandwiched by transversely isotropic solids or isotropic solids with the material constants given by Eqs. (21) and (22), respectively. The anisotropy in the solid strongly affects the wave characteristics, which may be useful for inverse analyses of the solid properties.

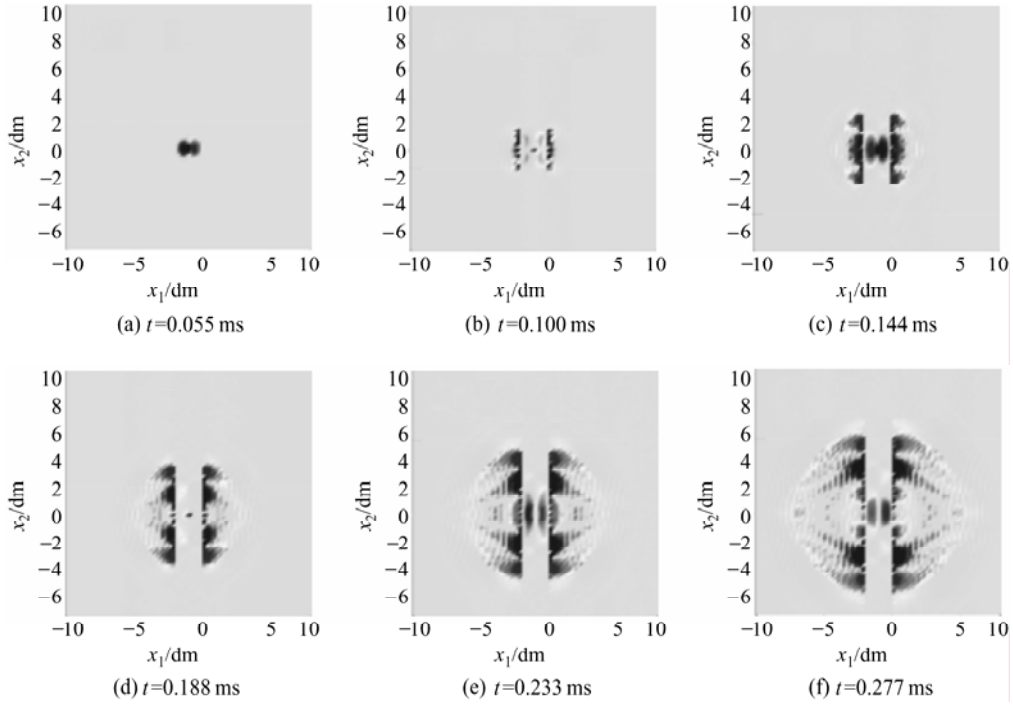

Fig. 6 Snapshots of acoustic and elastic waves around a dipole point source at several time steps

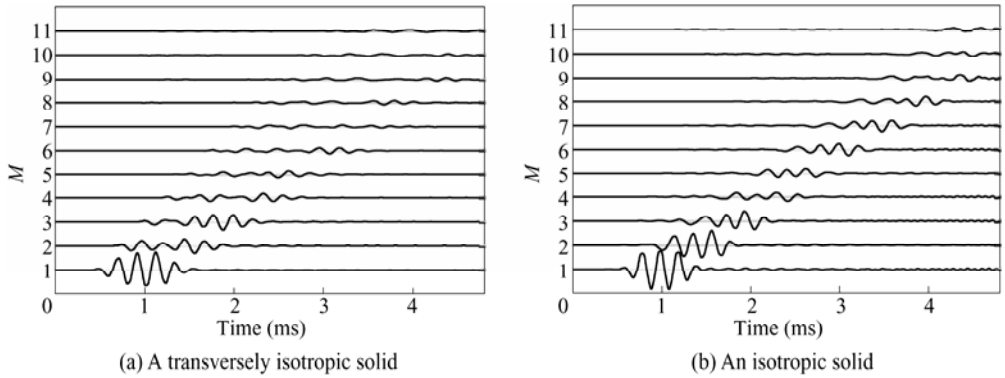

Fig. 7 Pressure waveforms at several points in a fluid sandwiched by (a) a transversely isotropic solid and (b) an isotropic solid. The source is a dipole with T_0 =0.2 ms.

5 Conclusions

The transient behavior of acoustic and elastic waves near a fluid and solid interface were obtained using the time domain boundary element method in conjunction with the fundamental solutions for general anisotropic solids. The numerical results allow detailed arrival identification and interpretation of acoustic and elastic

waves propagating along the fluid-solid interfaces. Though the numerical calculations in this study were done only for two-dimensional problems, three-dimensional problems with more realistic borehole models will be investigated in the near future.

References

[1] Sinha B K, Zeroug S. Geophysical prospecting using sonics and ultrasonics. In: Webster J G, ed. Wiley Encycl. Electrical and Electronics Engineering. John Wiley and Sons, Inc., 1999: 340-365.

[2] Yoon K H, McMechan G A. 3-D finite-difference modeling of elastic waves in borehole environments. *Geophysics*, 1992, **57**: 793-804.

[3] Cheng N, Cheng C H, Toksoz M N. Borehole wave propagation in three dimensions. *J. Acoust. Soc. Am.*, 1995, **97**: 3483-3493.

[4] Liu Q H, Schoen E, Daube F, et al. A three-dimensional finite difference simulation of sonic logging. *J. Acoust. Soc. Am.*, 1996, **100**: 72-79.

[5] Chen Y H, Chew W C, Liu Q H. A three-dimensional finite difference code for the modeling of sonic logging tools. *J. Acoust. Soc. Am.*, 1998, **103**: 702-712.

[6] Wang C Y, Achenbach J D. Elastodynamic fundamental solutions for anisotropic solids. *Geophys. J. Int.*, 1994, **118**: 384-392.

[7] Wang C Y, Achenbach J D, Hirose S. 2-D time domain BEM for scattering of elastic waves in solids of general anisotropy. *Int. J. Solids Struct.*, 1996, **33**: 3843-3865.

[8] Achenbach J D. Wave Propagation in Elastic Solids. Amsterdam: North-Holland Pub., 1973.

Professor Andrew Chi Chih Yao: Developing China's Computer Science

It was for Tsinghua University Professor Andrew Chi-chih Yao just a routine Thursday schedule. First he gave a lesson in the morning to the Pilot Computer Science class. With two foreign scholars, he conducted a seminar at 2:00 that afternoon for graduate students. By late that afternoon, Professor Yao was ready to turn to his own research. It was just a very common day for Tsinghua University's Professor Yao.

Professor Yao is a world-renowned computer scientist. He received the prestigious A. M. Turing Award in 2000 for his "fundamental contributions to the theory of computation, including the complexity-based theory of pseudo-random number generation, cryptography, and communication complexity". He has been on the faculty at such universities as MIT, Stanford, UC Berkeley, and Princeton. He left Princeton in 2004 to become a Tsinghua University Professor of Computer Science.

As a result of Professor Yao's efforts to build a world class presence computer science, Tsinghua now is able to attract leading students, scholars, and conferences in core computer science specialties. The 10th International Conference on Theory and Practice of Public Key Cryptography (PKC), for example, was held at Tsinghua from April 17 to 19, 2007. More than 100 cryptology experts from China and abroad participated in the three-day meeting. It was the first time the annual conference was held in China.

（From http://news.tsinghua.edu.cn，2007-07-19）